Probing Structure and Dynamics of DNA with 2-Aminopurine: Effects of Local Environment on Fluorescence†

Edward L. Rachofsky,‡ Roman Osman,§ and J. B. Alexander Ross*,‡

Department of Biochemistry and Molecular Biology and Department of Physiology and Biophysics, Mount Sinai School of Medicine, One Gustave L. Levy Place, New York, New York 10029

Received July 17, 2000; Revised Manuscript Received October 30, 2000

ABSTRACT: 2-Aminopurine (2AP) is an analogue of adenine that has been utilized widely as a fluorescence probe of protein-induced local conformational changes in DNA. Within a DNA strand, this fluorophore demonstrates characteristic decreases in quantum yield and emission decay lifetime that vary sensitively with base sequence, temperature, and helix conformation but that are accompanied by only small changes in emission wavelength. However, the molecular interactions that give rise to these spectroscopic changes have not been established. To develop a molecular model for interpreting the fluorescence measurements, we have investigated the effects of environmental polarity, hydrogen bonding, and the purine and pyrimidine bases of DNA on the emission energy, quantum yield, and intensity decay kinetics of 2AP in simple model systems. The effects of environmental polarity were examined in a series of solvents of varying dielectric constant, and hydrogen bonding was investigated in binary mixtures of water with 1,4-dioxane or *N*,*N*-dimethylformamide (DMF). The effects of the purine and pyrimidine bases were studied by titrating 2AP deoxyriboside (d2AP) with the nucleosides adenosine (rA), cytidine (rC), guanosine (rG), and deoxythymidine (dT), and the nucleoside triphosphates ATP and GTP in neutral aqueous solution. The nucleosides and NTPs each quench the fluorescence of d2AP by a combination of static (affecting only the quantum yield) and dynamic (affecting both the quantum yield and the lifetime, proportionately) mechanisms. The peak wavelength and shape of the emission spectrum are not altered by either of these effects. The static quenching is saturable and has half-maximal effect at approximately 20 mM nucleoside or NTP, consistent with an aromatic stacking interaction. The rate constant for dynamic quenching is near the diffusion limit for collisional interaction ($k_q \approx 2 \times 10^9$ M^{-1} s^{-1}). Neither of these effects varies significantly between the various nucleosides and NTPs studied. In contrast, hydrogen bonding with water was observed to have a negligible effect on the emission wavelength, fluorescence quantum yield, or lifetime of 2AP in either dioxane or DMF. In nonpolar solvents, the fluorescence lifetime and quantum yield decrease dramatically, accompanied by significant shifts in the emission spectrum to shorter wavelengths. However, these effects of polarity do not coincide with the observed emission wavelength-independent quenching of 2AP fluorescence in DNA. Therefore, we conclude that the fluorescence quenching of 2AP in DNA arises from base stacking and collisions with neighboring bases only but is insensitive to base-pairing or other hydrogen bonding interactions. These results implicate both structural and dynamic properties of DNA in quenching of 2AP and constitute a simple model within which the fluorescence changes induced by protein−DNA binding or other perturbations may be interpreted.

Local variations in the structure and dynamics of DNA can play important roles in mediating the protein−DNA interactions involved in many cellular processes. Characterization of such localized changes typically requires the use of spectroscopic methods in which a probe is incorporated into DNA at a specific site. Among the most widely utilized of such probes is 2-aminopurine (2AP),[1] a highly fluorescent isomer of adenine. 2AP possesses several desirable qualities as a fluorescence probe. First, the structure of DNA is minimally perturbed by replacement of adenine with 2AP, which can form a normal Watson−Crick base pair with thymine (*1*, *2*). Second, the fluorescence of this probe can be selectively excited in the presence of DNA, RNA, and proteins, because the absorption occurs at longer wavelengths than those of the nucleic acid bases and aromatic amino acids. Finally, the fluorescence of 2AP is strongly quenched within DNA, and this quenching is sensitive to local and global changes in DNA conformation. For all these reasons, this fluorophore has been employed as a probe of the structural and dynamic changes that characterize folding of ribozymes (*3*), DNA containing damage or mismatches (*4*, *5*), and the interactions of proteins with DNA, including DNA and RNA polymerases (*6*−*22*), restriction endonucleases (*23*−*25*), and repair enzymes (*26*−*32*).

† Supported by NSF Grant DBI-9724330 and NIH Grant CA63317.

* To whom correspondence should be addressed. Telephone: (212) 241−5569. Fax: (212) 996-7214. E-mail: ross@inka.mssm.edu.

‡ Department of Biochemistry and Molecular Biology.

§ Department of Physiology and Biophysics.

[1] Abbreviations: 2AP, 2-aminopurine; d2AP, 2-amino-9-deoxyribosylpurine; 3MI, 3-methylisoxanthopterin; DMF, *N*,*N*-dimethylformamide; TFE, 2,2,2-trifluoroethanol; rA, adenosine; rC, cytidine; rG, guanosine; dT, deoxythymidine; NTP, nucleoside triphosphate.

10.1021/bi001664o CCC: $20.00
Published on Web 01/03/2001

Despite the broad utilization of 2AP in biochemical and biophysical studies, little is understood about the molecular interactions that give rise to its fluorescence changes in DNA. These interactions could include hydrogen bonding and aromatic stacking, as well as changes in solvation due to enclosure of the base within the double helix. Developing an understanding of the effects of each of these interactions on the fluorescence properties of 2AP would enable a more sophisticated interpretation of spectroscopic measurements. We have employed a series of simple model systems to elucidate the effects of each of the aforementioned molecular interactions on the fluorescence spectrum, quantum yield, and emission decay kinetics.

Previous studies have revealed that both the lowest-energy ultraviolet absorption band and the fluorescence emission of 2AP can be attributed to a single excited state, which has $\pi\pi^*$ character (*33*). In neutral aqueous solution, the peaks of the absorption and emission spectra are observed at approximately 303 and 370 nm, respectively (*34*, *35*). The fluorescence quantum yield in aqueous solution has been estimated to be approximately 0.68, 3 orders of magnitude higher than those of the standard DNA bases (*36*). The fluorescence intensity decay kinetics are monoexponential, with reported lifetimes of approximately 12 and 10 ns for the free base and nucleoside, respectively (*37*). Changes in pH do not significantly change the peak absorption and emission wavelengths or intensity decay kinetics until relatively extreme values have been reached, implying that the fluorophore exists in a single protonation state in neutral solution (*36*, *37*).

In series of solvents of varying polarity, the peak absorption wavelength is essentially constant, varying only $\pm$ 3 nm (*34*, *35*). In contrast, the emission maximum shifts fairly sensitively to longer wavelength with increasing solvent polarity, ranging from 344 nm for 9-ethyl-2-aminopurine in cyclohexane to 370 nm for 2AP base and nucleoside in water (*34*−*36*). These shifts are consistent with standard theories of the effects of solvation on the electronic spectra of aromatic chromophores (*38*−*42*). They imply that the excited emitting state has a larger molecular dipole moment than the ground state, and that shifts in the emission spectrum could be employed to measure the polarity of the environment of the probe. However, these shifts could also arise in part from changes in specific chemical interactions, particularly hydrogen bonding, between solvents (*43*).

The fluorescence quantum yield shows a strong correlation with peak emission wavelength, increasing dramatically with increases in solvent polarity (*35*, *36*). This sensitivity to environmental polarity has been attributed to an intramolecular quenching mechanism, which has been postulated to be a vibronic coupling interaction of the emitting state with a close-lying $n\pi^*$ state (*35*). Such an $n\pi^*$ state has been observed with peak absorption at 278 nm (*33*). The dependence of this process on solvent polarity is believed to arise from the opposite shifts in the energies of these two excited states with solvent polarity. A recent quantum chemical study has demonstrated the presence of such an $n\pi^*$ state with electronic properties such that it would be destabilized both in polar solvents and by hydrogen bonding (*44*).

In both single-stranded (ss) and double-stranded (ds) DNA, the emission spectrum of 2AP is shifted less than 1 nm from its position in neutral buffer (*34*). The quantum yield is significantly reduced, and varies between oligonucleotides (oligos) of differing sequence (*5*, *14*, *24*). The intensity decay kinetics in DNA are not single exponential but can be fitted empirically to sums of three or four exponential terms. In these analyses, the number- and intensity-averaged lifetimes (which are defined in Materials and Methods below) are consistently less than those of the free base and nucleoside. Aromatic stacking interactions have been suggested as the basis for the changes in both quantum yield and average lifetime (*45*, *46*). However, this hypothesis has not been tested in a rigorous fashion, and no physical model describing the mechanisms giving rise to the complex decay kinetics has been established.

Changes also have been reported in the absorption spectrum of 2AP in DNA relative to that in aqueous buffer (*4*, *45*, *46*). Two distinctive features have been observed. First, excitation energy transfer has been observed from normal DNA bases to 2AP in both ssDNA and dsDNA. The efficiency of this process decreases with increasing temperature (*45*, *46*). For 2AP opposite an abasic site, the transfer efficiency also decreases in concert with an apparent movement of the fluorescent base to an extra-helical conformation (*4*). On the basis of these results, excitation transfer has been proposed to occur in a stacked complex of 2AP and neighboring bases, which is disrupted by increasing temperature or by conformational change (*45*). In ssDNA, this energy transfer is much more efficient from adenine (A) than from the other DNA bases, consistent with a recent report that single-stranded poly-A is stacked while other ssDNA is not (*47*). Second, the fluorescence excitation spectrum for direct excitation of 2AP has been observed to shift to longer wavelength in DNA (*46*). This spectral shift demonstrates identical dependences on temperature, sequence context, and base conformation as the excitation transfer (and indeed has been observed in the same oligos). This shift has been attributed to a general solvation effect resulting from changes in exposure of the fluorophore to solvent water (*46*). However, the magnitude of this absorption shift is significantly greater than the modest spectral shifts observed in pure solvents, suggesting that the sensitivity of 2AP absorption to the general solvent effect is insufficient to account for the change in excitation energy. It seems more likely that this shift arises from perturbation of the electronic structure of the excited-state fluorophore by formation of a stacked complex. One possible description of this perturbation has been suggested by a recent quantum chemical calculation of 2AP stacked with thymine (T), which predicted a new lowest-energy excited-state having the character of a charge-transfer (CT) from 2AP to T (*48*).

Finally, there has been a single report suggesting that the quenching of 2AP fluorescence in DNA is dominated by distance-dependent electron transfer from 2AP to G (*49*). However, this model has not been verified by any direct observation of 2AP-G electron transfer. Furthermore, this mechanism alone cannot explain all of the reported dependence of 2AP lifetime and quantum yield on DNA sequence context. For example, at 4 °C the intensity-averaged fluorescence lifetime of 2AP in a 7-mer with a central GG(2AP)GG sequence is 6.5 ns (*5*); at the same temperature, 2AP in a 10-mer with a central GA(2AP)TT sequence has an intensity-averaged lifetime of 4.5 ns (*24*). Clearly, other factors beside the proposed 2AP-G electron transfer must

be determinants of fluorescence quenching in DNA.

On the basis of the previous results in both oligos and pure solvents, we perceive three factors that could contribute to the changes in 2AP quantum yield, lifetime, and intensity decay kinetics in DNA. These factors are aromatic stacking, hydrogen bonding, and general solvation. We investigate each of these factors using simple model systems. The effects, including stacking, of the nucleic acid bases are determined from titrations of 2AP deoxyriboside (d2AP) with nucleosides and NTPs in aqueous buffer. The effects of general solvation and hydrogen bonding are investigated by measurement of emission wavelength, quantum yield, and intensity decay in neat solvents and binary solvent mixtures, respectively. The results indicate the pre-eminent importance of the flanking bases in 2AP quenching. These bases exert their effects through both stacking and collisional quenching mechanisms, each of which is a significant contributor to the observed decrease in quantum yield. Hydrogen bonding and solvation are demonstrated to contribute negligibly to the fluorescence quenching. These results serve as the basis for a model enabling the interpretation of specific fluorescence changes in terms of the structure and dynamics of DNA.

MATERIALS AND METHODS

Materials. 2AP, rA, rC, rG, dT, ATP, and GTP were purchased from Sigma and used without further purification. d2AP was the gift of Professor Lawrence C. Sowers (City of Hope National Medical Center). Aqueous solutions of 2AP, d2AP, and nucleosides were prepared in a buffer of 20 mM tris·HCl, 60 mM NaCl, and 0.1 mM Na_2EDTA, with pH adjusted to 7.5 by addition of HCl. Aqueous solutions of NTPs and aqueous/glycerol mixtures were prepared in a buffer of 200 mM tris·HCl, 60 mM NaCl, and 0.1 mM Na_2-EDTA, pH 7.5. 1,4-Dioxane (Pierce), *N*,*N*-dimethylformamide (Sigma), ethanol (Pierce), trifluoroethanol (TFE) (Sigma), and glycerol (Mallinckrodt) were each the highest grade available.

Samples and Titrations. Nucleoside and NTP titrations were performed by serial addition of aliquots of maximally concentrated nucleoside (NTP) stock to the starting solution, where both solutions contained equal concentrations (~10 μM) of d2AP. All stock solutions were prepared in the aqueous buffers described above. Concentrations were estimated from UV absorption spectra obtained using a Hitachi U-3210 UV/vis dual beam spectrophotometer. Extinction coefficients at neutral pH were taken to be the following: 2AP and d2AP: $\epsilon_{303\ nm} = 6000\ M^{-1}\ cm^{-1}$ (*50*); rA: $\epsilon_{260} = 15\ 100\ M^{-1}\ cm^{-1}$; ATP: $\epsilon_{260} = 15400\ M^{-1}\ cm^{-1}$; rC: $\epsilon_{271} = 9100\ M^{-1}\ cm^{-1}$; rG and GTP: $\epsilon_{252.5} = 13\ 700\ M^{-1}\ cm^{-1}$; dT: $\epsilon_{267} = 9700\ M^{-1}\ cm^{-1}$ (*51*). To further elucidate the kinetics of these interactions, the viscosity of solutions containing d2AP and several concentrations of dT was incremented by addition of various quantities of glycerol to aqueous buffer. These glycerol−water mixtures were prepared by weight, and the viscosities were determined by reference to a standard table (*52*).

The organic solvents dioxane, DMF, ethanol, and TFE were each poured from a freshly opened bottle, and all working stocks and samples were stored under argon. These solvents demonstrated negligible background fluorescence, and their ultraviolet absorbance did not change over the course of the experiments. Binary solvent mixtures of water with dioxane or DMF were generated by serial addition of aliquots of aqueous buffer into the organic solution, with equal concentrations of 2AP (~10 μM) present in both solvents. No correction was made for the effects of nonideal mixing on the specific volume of the solution. All titrations were performed directly in cuvettes and mixed by inversion.

Steady-State Fluorescence Spectroscopy. Fluorescence spectra were obtained for samples in $10 \times 10\ mm^2$ quartz fluorescence cuvettes using an SLM 4800 spectrofluorometer that had been modified for single photon counting detection. Excitation was at 309 nm and emission was detected over the range of 320 to 480 nm, with a 4-nm band-pass for each. At this excitation wavelength, the absorbance and fluorescence of all sample components (nucleosides, solvents, buffer salts, etc.) except 2AP were negligible. The excitation polarizer was set to 54.7° from vertical (the magic angle) (*53*) and the emission polarizer was set to the vertical position to collect photons under magic angle conditions while minimizing the Wood's anomaly of the monochromators. Emission spectra were corrected for the nonlinear response of the fluorometer using a standard curve derived from absolute emission spectra of several model compounds. Spectral intensities were obtained by integrating the emission spectra over the entire wavelength range. The average emission wavelength was taken to be the center-of-gravity of the emission spectrum:

$$C/G = \sum \nu F(\nu) / \sum F(\nu) \qquad (1)$$

where ν represents wavenumber (inverse wavelength), and $F(\nu)$ is the fluorescence intensity at that wavenumber.

Time-Resolved Fluorescence Spectroscopy. Fluorescence intensity decay measurements were performed by the method of time-correlated single-photon counting (TCSPC) (*54*). Samples were excited by short (~2 ps full-width at half-maximum) pulses of vertically polarized laser light. The laser system was a frequency-doubled diode laser (Coherent Verdi V-10), operating at 532 nm, pumping a Ti:sapphire laser (Coherent Mira 900), which was tuned to lase at 927 nm and mode-locked at 76 MHz. A pulse picker (Coherent 9200) reduced the laser repetition rate to 4.8 MHz. The light was then passed through a frequency tripler (Inrad 5-050) to generate 309-nm pulses for excitation. The emission first passed through a polarizer oriented at the magic angle. Fluorescence emission was detected at 360 nm using a monochromator with a band-pass of 20 nm, and photons were collected by a microchannel plate photomultiplier tube (Hamamatsu R2809U-06). The instrument response function was detected at 313 nm using light scattered by a dilute suspension of colloidal silica. The sample chamber, collection optics, and timing electronics have been described previously (*55*). Decay curves were collected into either 1000 or 2000 channels with timing calibration of 40 or 20 ps/channel, respectively. Data collection was terminated for samples in neat solvents and titration endpoints when 40 000 counts were in the peak channel and for the middle points of titrations at 20 000 peak counts.

Time-resolved fluorescence data were analyzed by a standard reconvolution procedure (*56*) using nonlinear regression (*57*). The fluorescence intensity decay was fit to

a sum of exponentials:

$$I(t) = \sum_{i=1}^{n} \alpha_i e^{-t/\tau_i} \quad (2)$$

where the preexponential factors α_i are the amplitudes of each component, and τ_i are fluorescence lifetimes. Certain analyses of titration data were performed using a global procedure with lifetimes τ_i as common parameters (*58*, *59*). In cases where a single-exponential term was not adequate to fit the observed kinetics, number-averaged and intensity-averaged fluorescence lifetimes (*54*) were computed, respectively, according to

$$\tau_{num} = \sum_{i=1}^{n} \alpha_i \tau_i / \sum_{i=1}^{n} \alpha_i \quad (3)$$

$$\tau_{int} = \sum_{i=1}^{n} \alpha_i \tau_i^2 / \sum_{i=1}^{n} \alpha_i \tau_i \quad (4)$$

The value of τ_{num} is proportional to the area under a steady-state spectrum (in the absence of static quenching). The value of τ_{int} represents the average time that a fluorophore exists in the excited state.

Nucleoside and NTP Titration Analysis. Fluorescence lifetimes from nucleoside and NTP titrations were fitted to the Stern−Volmer equation for analysis of collisional quenching:

$$\tau_0/\tau = 1 + k_q \tau_0 [Q] \quad (5)$$

where τ_0 and τ are the lifetimes in the absence and presence of quencher, respectively, [*Q*] is the nucleoside (NTP) concentration (M), and k_q is the bimolecular quenching rate constant (M^{-1} s^{-1}) (*53*). When more than one exponential term was required to fit an intensity decay curve, the intensity-averaged lifetime was employed for Stern−Volmer analysis.

Fluorescence intensity decay data for some nucleoside titrations also were fit to a transient diffusional model:

$$I(t) = I_0 e^{-t/\tau_0} e^{-4\pi N_A \gamma \sigma D[Q](t + [(2\sigma)/(\sqrt{\pi D})]t^{1/2})} \quad (6)$$

where N_A is Avogadro's number, D is the diffusion coefficient (cm^2/s) of the nucleoside, σ is the encounter distance (Å) for collisional quenching, and γ is the intrinsic efficiency of the quenching interaction (*60*, *61*). This model assumes that quenching occurs not through a collision of hard-sphere type molecules but when a quencher approaches within a distance σ of the fluorophore. Significant deviations from exponential decay kinetics result when a population of quencher molecules is within σ of the fluorophore at the time of excitation. As eq 6 shows, the degree of nonexponential character increases with increasing σ or decreasing D. Global analysis was also applied in these analyses, with D, σ, and γ as common parameters.

Steady-state fluorescence intensity data for nucleoside and NTP titrations was analyzed according to a model of combined static and dynamic quenching:

$$F_0/F = (1 + k_q \tau_0 [Q])(1 + K_a [Q]) \quad (7)$$

where K_a is the association constant (M^{-1}) for the formation of a binary complex between the fluorophore (d2AP) and the quencher (nucleoside) (*62*). In this model, static quenching of fluorescence arises from formation of a nonemissive complex with quencher when the fluorophore is in its electronic ground state. The fractional binding saturation $Y = [FQ]/([F] + [FQ])$ at each quencher concentration can be expressed as

$$Y = 1 - \left(\frac{\tau_0}{\tau}\right)\left(\frac{F_0}{F}\right)^{-1} \quad (8)$$

For analyses by eq 7, k_q and τ_0 were fixed to the values obtained from time-resolved experiments to reduce the uncertainty in cross-correlated kinetic parameters.

RESULTS

Nucleoside and NTP Titrations I. Static and Dynamic Quenching. Within a DNA strand, adjacent bases can form complexes by aromatic stacking and also may experience collisions. Both the stacking and the collisional interactions could give rise to quenching of an incorporated fluorescent base such as 2AP. Because each of these interactions also can occur when bases are free in solution, it is possible to investigate their effects on the fluorescence emission spectrum, quantum yield, lifetime, and decay kinetics of 2AP by titrating this fluorophore with increasing concentrations of the nucleic acid bases. In practice, these titrations are best performed with nucleosides or NTPs because the free bases are sparingly soluble in water. Therefore, we have titrated d2AP with the nucleosides rA, rC, rG, and dT, and the nucleoside triphosphates ATP and GTP. Use of all four nucleosides permits comparison of their intrinsic ability to quench fluorescence, and comparison with the NTPs investigates the effect of the phosphate charges on the base interactions.

Both the fluorescence quantum yield and the intensity decay lifetime of d2AP decrease with increasing concentration of nucleoside or NTP in aqueous buffer at pH 7.5. The changes in steady-state fluorescence intensity and intensity-averaged lifetime τ_{int} for d2AP with increasing [dT] are shown in the Stern−Volmer plot in Figure 1A (the decay kinetics are discussed below). The ratio of lifetimes in the absence and presence of dT, τ_0/τ, is linear with increasing [dT], consistent with a collisional quenching process. Fitting of the lifetime data to eq 5 yields a quenching rate constant k_q of $2.14 \pm 0.04 \times 10^9$ M^{-1} s^{-1}. This value is close to the theoretical limit for the collisional rate constant for these two molecules, indicating that collisional quenching of d2AP by dT is intrinsically a highly efficient process.

The steady-state fluorescence decreases more markedly than the lifetime upon addition of dT. In the absence of any static quenching process, the change in steady-state fluorescence intensity with increasing [*Q*] would be proportional to the change in τ_{num}. However, as is shown in Figure 1, panel A, F_0/F demonstrates significant upward curvature on the Stern−Volmer plot. This result indicates that there is a static component to the quenching of d2AP by dT. The static quenching may arise due to the reversible formation of a complex between the fluorophore and the quencher while the fluorophore is in the electronic ground state. If this reaction involves formation of a binary complex only

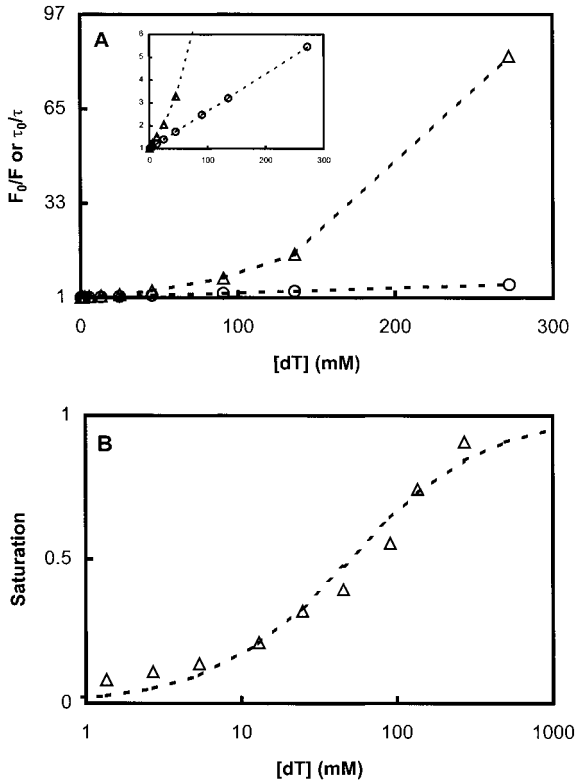

FIGURE 1: Quenching of d2AP by dT. (A) Stern−Volmer plot of F_0/F (triangles) and τ_0/τ (circles) vs [dT]. The inset shows an expansion of the ordinate axis; (B) Fractional saturation of dT:d2AP binding interaction. The points represent experimental values; the line represents the best fit of eq 8 to these values.

(F + Q ⇌ FQ), the change in fluorescence intensity can be described by eq 7. Fitting of the steady-state data in Figure 1, panel A, to eq 7 yields an apparent association constant of 54 M^{-1}, corresponding to a Gibbs free energy of binding of −2.4 kcal/mol at 298 K. Both the experimental and the fitted values of the fractional binding saturation *Y* for this complex are shown in Figure 1, panel B, and demonstrate good agreement. As Figure 1, panel B, shows, more than 80% of the d2AP appears to be bound by dT at the titration endpoint.

The association constant and free energy derived for d2AP:dT binding are within the range previously reported for the stacking association of 2AP and other aromatic chromophores (*63*−*66*). Therefore, we attribute the static quenching to the formation of a stacked complex between the aromatic bases of d2AP and dT. This complex, which could also exist in DNA, is nonfluorescent and consequently does not contribute to the intensity decay. Of course, the thermodynamic cycle for the stacking interaction may include higher-order assembly states besides the binary complex. However, the populations and stoichiometries of these possible states cannot be inferred from the current data, and the binding isotherm is empirically fit by a two-state model.

In other systems, positive curvature in Stern−Volmer plots sometimes has been attributed to so-called "sphere-of-action" quenching (*62*). However, this model generally predicts deviations from ideal collisional quenching only at much higher [*Q*] than is observed here. Therefore, the "sphere-of-action" model does not appear to provide an adequate explanation of the observed quenching data.

Table 1: Static and Dynamic Quenching Parameters for Nucleosides and NTPs

nucleoside	k_q ($\times 10^9$ M^{-1} s^{-1})	K_{SV} (M^{-1})	K_a (M^{-1})	ΔG (kcal/mol)	Y_{max}[a]
dT	2.14 ± 0.04[c]	21.8[d]	*e*	*e*	0.36
dT[b]	1.90 ± 0.01	16.3	54 ± 10	−2.4	0.85
rA	2.21 ± 0.10	22.5	*e*	*e*	0.16
rC	1.90 ± 0.03	19.4	*e*	*e*	0.38
rG	1.70 ± 0.13	17.8	*e*	*e*	0.10
ATP[b]	1.91 ± 0.10	16.3	32 ± 10	−2.1	0.76
GTP[b]	1.79 ± 0.07	15.3	32 ± 10	−2.1	0.81

[a] Saturation at maximal [nucleoside (NTP)] as estimated from eq 8. [b] Performed in a buffer of 200 mM tris·HCl, 60 mM NaCl, 0.1 mM Na_2EDTA, pH 8. Unless so noted, other titrations were performed in a buffer of 20 mM tris·HCl, 60 mM NaCl, 0.1 mM Na_2EDTA, pH 8. [c] For each titration, uncertainties in k_q were determined from least-squares data fitting. Reported uncertainties are derived from averaging recovered values of k_q and K_a for repeat titrations. [d] Stern−Volmer constants K_{SV} calculated based on τ_0 = 10.2 ns for d2AP, except in 200 mM tris buffer, where τ_0 = 8.6 ns. [e] K_a and ΔG not computed because insufficient binding saturation was obtained at the maximum [nucleoside].

The three other nucleosides rA, rC, and rG demonstrate static and dynamic quenching properties that are essentially similar to that of dT. For all of these nucleosides, the Stern−Volmer plot for lifetime data is linear, while that for steady-state fluorescence shows upward curvature. Moreover, the k_q values all are within 30% of each other; the lowest k_q is 1.70 ± 0.10 × 10^9 M^{-1} s^{-1} for rG, and the highest is 2.21 ± 0.10 × 10^9 M^{-1} s^{-1} for dA. These values are summarized in Table 1. The reported uncertainties are derived from fitting the data to eq 5; k_q values derived from repeat titrations agreed to within 10%. The upward curvature in the Stern−Volmer plots of steady-state fluorescence data indicates that all of the nucleosides quench 2AP by both static and dynamic mechanisms. The association constants for formation of a statically quenched complex between d2AP and each of the other three nucleosides cannot be determined, however, because the solubilities of rA, rC, and rG are less than that of dT; the estimated fractional binding saturation at each of the titration endpoints is less than 0.5, so K_a values cannot be determined with any certainty. Nevertheless, each Stern−Volmer plot shows similar upward curvature at the same nucleoside concentration, implying that the equilibrium constant for formation of these complexes is approximately equal to that for the complex of dT and d2AP.

The NTPs ATP and GTP show similar static and dynamic quenching behavior to the four nucleosides. For the dynamic quenching, the k_q values derived from lifetime data (Table 1) are in the same range as for the corresponding nucleosides. In measurements of static quenching, binding saturations of greater than 0.75 can be achieved for both ATP and GTP, consequently enabling calculation of K_a for the d2AP:NTP interactions (*67*). As shown in Table 1, the association constants and binding free energies are close to the respective values for dT. Therefore, it may be concluded that the presence of the triphosphate group does not interfere with either the stacking or collisional interactions.

The emission spectrum does not change in either center-of-gravity (C/G) (eq 1; an averaged measure of peak wavelength) or shape with addition of any nucleoside or NTP. This invariance is expected for collisional quenching (*62*). Although the formation of a stacked complex might

Table 2: Multiple Exponential Fits of d2AP Intensity Decays as a Function of [dT]

[dT] (mM)	α_1	α_2	α_3	τ_1 (ns)	τ_2 (ns)	τ_3 (ns)	τ_{int} (ns)	τ_{num} (ns)
0			1.000			8.58	8.58	8.58
1.4			1.000			8.42	8.42	8.42
2.7			1.000			8.22	8.22	8.22
5.3			1.000			7.90	7.90	7.90
13			1.000			7.09	7.09	7.09
25			1.000			6.12	6.12	6.12
45		0.062	0.938		1.23	4.99	4.93	4.75
91		0.102	0.898		1.00	3.55	3.29	3.47
136	0.210	0.098	0.692	0.13	1.01	2.79	2.67	2.06
272	0.326	0.154	0.520	0.09	0.62	1.73	1.58	1.02
0 (1 cp)[a]			1.000			8.58	8.58	8.58
0 (2 cp)			1.000			9.10	9.10	9.10
0 (3 cp)			1.000			9.21	9.21	9.21
0 (4 cp)			1.000			9.21	9.21	9.21
0 (5 cp)			1.000			9.21	9.21	9.21
150 (1 cp)	0.206	0.099	0.695	0.17	1.13	2.70	2.56	2.02
150 (2 cp)	0.237	0.084	0.679	0.22	1.57	4.54	4.36	3.27
150 (3 cp)	0.229	0.082	0.688	0.30	1.96	5.61	5.38	4.09
150 (4 cp)	0.228	0.092	0.680	0.27	1.65	6.09	5.85	4.35
150 (5 cp)	0.213	0.095	0.692	0.27	1.77	6.35	6.10	4.62

[a] Viscosity (cp) of aqueous glycerol mixtures is indicated in parentheses. The viscosities correspond to percent (w/w) glycerol in aqueous solution according to 1 cp: 0%; 2 cp: 24%; 3 cp: 35%; 4 cp: 41%; 5 cp: 46%. The aqueous buffer for all listed samples consisted of 200 mM tris·HCl, 60 mM NaCl, 0.1 mM Na_2EDTA, pH 7.5.

change the relative energies of the ground and excited states, such an effect cannot be observed in the emission spectrum because the stacked complex is nonemissive.

Nucleoside and NTP Titrations II. Decay Kinetics. The fluorescence intensity decay of d2AP in the absence of nucleoside or NTP displays single-exponential kinetics with $\tau = 10.2$ ns, in excellent agreement with previous reports (*5*, *37*). At low nucleoside or NTP concentration, this monoexponential decay persists. However, at higher nucleoside or NTP concentration, the decay kinetics are no longer well-described by a single exponential model but require two or three exponential terms to fit adequately. The extent of the deviation from single exponential kinetics increases monotonically with increasing nucleoside or NTP concentration. The results of these multiexponential fits are summarized in Table 2 for titration of d2AP with dT.

Deviations from pure exponential decay kinetics at high concentrations of fluorescence quencher have been described by a "transient diffusional" model (*60*, *61*). In this model, quenching occurs whenever a quencher enters within a distance σ of the fluorophore. As [Q] increases, the probability increases that a quencher will be within σ of the fluorophore at the time of excitation. Under these conditions, the quenching rate constant will differ transiently from the homogeneous diffusional result by a factor proportional to $t^{-1/2}$, and consequently the fluorescence intensity decay will deviate from pure exponential behavior. As eq 6 shows, the extent of the deviation will increase with increasing encounter distance σ and decrease with increasing quencher diffusion coefficient D.

We hypothesize that the nonexponential fluorescence intensity decay kinetics of d2AP at high nucleoside or NTP concentration might arise from such a transient effect. To investigate this possibility, we examined the effect on the decay kinetics of varying solution viscosity, which should change D. Viscosity was incremented by addition of glycerol to aqueous solutions of d2AP at a constant [dT]. These titrations were performed in a buffer of 200 mM tris·HCl, 60 mM NaCl, and 0.1 mM Na_2EDTA, pH 7.5, to minimize changes in the proton activity of the solution due to increasing fraction of glycerol. In the absence of dT, the (monoexponential) lifetime of d2AP is 8.6 ns in this buffer (as compared to 10.2 ns in 20 mM tris·HCl), suggesting that there is weakly efficient quenching by tris base. Neither k_q nor K_a for the d2AP:dT interaction differs between the two buffers. With increasing glycerol, the steady-state fluorescence intensity and lifetime increase marginally (7%) between aqueous buffer and 46% (w/w) glycerol (which has a viscosity of 5 cp). The small increase in lifetime can be attributed to a decrease in quenching by tris base due to both increasing viscosity and decreasing [tris]. In the presence of 150 mM dT, the intensity decay is not monoexponential at any percent glycerol. The average lifetimes τ_{num} and τ_{int} increase much more dramatically with increasing glycerol than the single exponential lifetime does in the absence of dT. Between buffer and 46% glycerol, each of the average lifetimes increases approximately 250%, as is summarized in Table 2. These results indicate that increasing viscosity decreases the rate of d2AP dynamic quenching by dT, consistent with a reduction in the collisional interaction.

To test whether these decays could be described by the transient diffusional quenching model, data sets at 150 mM dT and various mass fractions of glycerol were fit globally to eq 6. In this analysis, I_0, γ, σ, and D were iterated parameters, γ and σ were common parameters for all data sets, and D was required to maintain an inverse (Stokes−Einstein) dependence on viscosity (*68*). At each mass fraction of glycerol, τ_0 was fixed to the value determined in the absence of dT. By using global analysis, which reduces the cross-correlation between iterated parameters and consequently increases the ability of nonlinear regression to reject incorrect models (*58*, *59*), we find that the decay kinetics are well-described by eq 6. The recovered parameters ($\gamma = 1.0$, $\sigma = 3.0$ Å, and $D = 6.8 \times 10^{-6}$ cm^2/s at 1 cp) are physically reasonable. Therefore, we conclude that the transient diffusional model is consistent with the observed decays. Of course, there are numerous other mechanisms that can give rise to nonexponential fluorescence decay kinetics. However, it seems reasonable to accept the transient diffusional model in this case because it requires invoking no other processes besides collisional quenching and because it fits decay data collected as a function of viscosity acceptably in a global analysis. The lack of any emission spectral shift also is consistent with the transient diffusional model invoked to describe the nonexponential intensity decay kinetics. The other mechanisms that could give rise to complex decay kinetics (e.g., ground-state heterogeneity or an excited-state reaction) would typically predict a change in the energy of the excited state (*62*), and such a shift is not observed.

In summary, the nucleoside and NTP derivatives of the four common aromatic bases of DNA efficiently quench the fluorescence of d2AP by a combination of static and dynamic effects. The nucleoside or NTP concentration dependence of static quenching is consistent with a mechanism of ground-state complex formation mediated by aromatic stacking interactions. The dynamic quenching is a collisional process

with a rate constant near the limit expected for free diffusion. The fluorescence intensity decay of d2AP in the presence of high nucleoside or NTP concentration is not monoexponential and is well-described by an extension of the theory of collisional quenching to include transient effects.

Solvation and Hydrogen Bonding Effects. In DNA, 2AP can participate in a number of hydrogen bonding interactions, including both base pairing and bonding with water molecules in the major and minor grooves. In principle, the stabilizing energy of any of these hydrogen bonds could be small enough that both bound and unbound states are significantly populated at equilibrium. Furthermore, the hydrogen bonding energy could change with excitation of the fluorophore, in which case the populations could change on the same time scale as emission. The effects of hydrogen bonding on the fluorescence properties of 2AP can be investigated in a mixed-solvent experiment, in which the interactions are titrated by addition of small quantities of a hydrogen bonding solvent to the fluorophore in a non-hydrogen bonding solvent. Of course, changing the composition of the solvent is expected to affect the fluorescence not only because of changes in hydrogen bonding but also because of changes in nonspecific (general) solvation (*69*). Therefore, interpretation of mixed-solvent experiments requires an understanding of general solvent effects as well. Such effects may also be important in DNA, where the base is partially buried in a hydrophobic environment. Solvation effects on fluorescence can be studied in a series of neat solvents of known polarity.

Several approximate theoretical models exist to predict the wavelength shifts in fluorescence spectra with solvent polarity (*38*−*42*). All of these models are alike in that they are based on a simplified picture of the fluorophore as a point dipole occupying a cavity within a continuum solvent and employ classical electrodynamics to estimate the energy of solvation. The energy shift in the emission spectrum is given in the simplest formulation as

$$\Delta E = \frac{2\vec{\mu}_e(\vec{\mu}_g - \vec{\mu}_e)}{a^3}\left(\frac{\epsilon - 1}{2\epsilon + 1} - \frac{n^2 - 1}{2n^2 + 1}\right) \qquad (9)$$

where $\vec{\mu}_g$ and $\vec{\mu}_e$ are the permanent dipoles of the ground and excited states, respectively, ϵ is the solvent dielectric constant, n is the refractive index, and a is the radius of the solute cavity (*40*). We will refer to the term in large parentheses as $f(\epsilon,n)$. This formulation includes only the effects of the permanent dipoles of the solvent on the spectral energy; other models also have included induced-dipole effects and dispersive interactions (*39*, *42*). Equation 9 demonstrates two common features of all of these models: first, that the energy shift is linearly proportional to some function $f(\epsilon,n)$, and second, that the molecular dipoles cannot be determined absolutely from experimental spectral shifts alone because the energy depends sensitively on the unknown parameter a. Therefore, these models are best employed as qualitative descriptions of the interactions underlying the solvent shifts, rather than as formulas for accurate calculation of molecular dipoles.

Lifetimes and Spectral Shifts in Neat Solvents. To assess the effects of solvent polarity on fluorescence lifetime and decay kinetics, we measured emission spectra and intensity decays in a series of neat solvents of varying $f(\epsilon,n)$. The emission spectra generally are shifted to longer wavelength with increasing solvent polarity without any change in spectral shape. As depicted in Figure 2, panel A, the emission C/G (eq 1) is well-correlated with $f(\epsilon,n)$, although these quantities do not obey the linear correspondence predicted by classical solvation theory (eq 9). The spectral shifts observed here agree well with previously reported values (*34*−*36*). The intensity decays are monoexponential in dioxane, DMF, ethanol, and aqueous buffer. In TFE, three exponential terms are required to fit the intensity decay data. No model is proposed to describe these kinetics; however, for the purpose of analyzing general solvent effects, it was assumed that the longest lifetime represents the emission of the base as a monomer free of any specific solvent interactions. This assumption is justified by the very large value of this lifetime (15.3 ns), which suggests that the corresponding emitting state undergoes essentially no quenching interactions. This long lifetime is accompanied by the largest red-shift in emission wavelength ever reported for this fluorophore (C/G = 385.7 nm, $\lambda_{max} \sim 375$ nm), consistent with the large $f(\epsilon,n)$ for TFE. As depicted in Figure 2, panel B, the fluorescence lifetime and the mean emission wavelength are well correlated with each other between neat solvents. This correlation holds even when there is relatively little

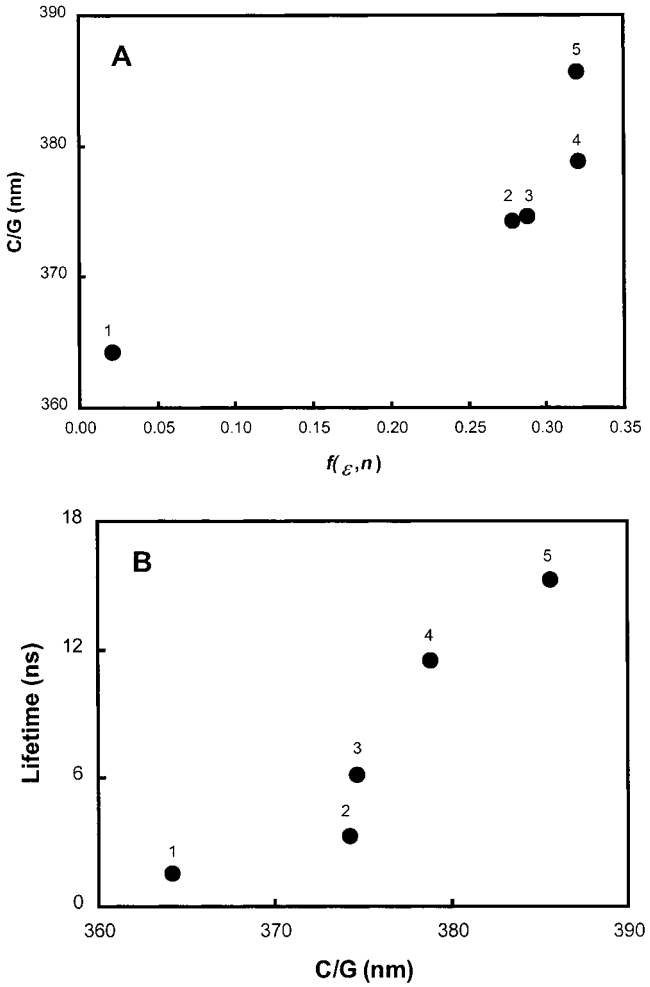

FIGURE 2: 2AP fluorescence properties in neat solvents. (A) Center-of-gravity (C/G) (eq 1) of corrected emission spectra vs solvent response function $f(\epsilon,n)$ (the term in parentheses in eq 9); (B) Fluorescence lifetime vs $f(\epsilon,n)$. In each panel, the numbered data points represent solvents as follows: 1, dioxane; 2, DMF; 3, ethanol; 4, water; 5, TFE.

change in $f(\epsilon,n)$. For example, large correlated changes in lifetime and emission wavelength between water and TFE are evident even though $f(\epsilon,n)$ changes very little: C/G shifts by over 6 nm to longer wavelength and τ increases by almost 4 ns. The lifetimes observed here agree well with previously reported relative quantum yields in dioxane, DMF, ethanol, and water (*35*, *36*). The observed wavelength−lifetime correlation is consistent with the previously proposed vibronic coupling mechanism of fluorescence quenching (*44*).

On the basis of the sensitivity of 2AP emission wavelength to solvent polarity, the absence of a significant spectral shift between water and DNA (*34*) suggests that there is little change in the efficiency of quenching mechanisms that are sensitive to general solvent effects. In other words, the base fluorescence should be quenched no more by these mechanisms in DNA than it is in water. Therefore, it may be concluded that these solvent-dependent quenching mechanisms, which may consist of vibronic coupling or other unspecified interactions, do not contribute significantly to the quenching of 2AP fluorescence in DNA. The mechanism of quenching in DNA must involve some other mechanism(s) that can occur independent of changes in solvation.

Binary Solvent Titrations. In a mixed solvent, the fluorescence emission wavelength, quantum yield, and intensity decay lifetime will vary between the values measured in the two neat solvent endpoints. For an ideal mixture of two solvents, neither of which interacts specifically with the fluorophore, the spectral shift will depend linearly on the mole fraction of each (*69*, *70*). Deviations from this linear behavior can be caused by multiple factors, including nonideal mixing, preferential solvation, or specific interactions between the fluorophore and one or both of the solvents (*71*). Each of these phenomena gives rise to a characteristic type of deviations from linearity. Specific interactions such as hydrogen bonding typically give rise to negative curvature in a plot of emission wavelength against mole fraction of the hydrogen bonding solvent (x_H), representing the saturable formation of hydrogen bonds with the fluorophore (*69*). This curvature is commonly observed at low x_H because for most solvent mixtures even $x_H \sim 0.1$ corresponds to a molar concentration sufficient to saturate these binding sites.

We investigated the effects of hydrogen bonding on the fluorescence properties of 2AP in binary mixtures of water with each of the non-hydrogen bonding solvents dioxane and DMF. The changes in emission C/M, relative fluorescence quantum yield, and intensity decay lifetime with increasing mole fraction of water (x_w) in dioxane and DMF are displayed in Figure 3. Each of these quantities increases monotonically with increasing x_w. The C/M (Figure 3, panel A) depends approximately linearly on x_w in both organic solvents, although in dioxane there is some curvature at both the low and high ends of the curve. The relative quantum yield (Figure 3, panel B) and lifetime (Figure 3, panel C) also depend nearly linearly upon x_w, although there is some slight curvature to each plot. The intensity decay is monoexponential in each solvent mixture.

The ratio of quantum yield to lifetime is constant upon addition of water to DMF, indicating that there is no change in static quenching. However, the relative quantum yield and lifetime do not change proportionately between dioxane and water. The relative quantum yield is 5-fold greater in water than in dioxane, but the lifetime is 8-fold greater. These

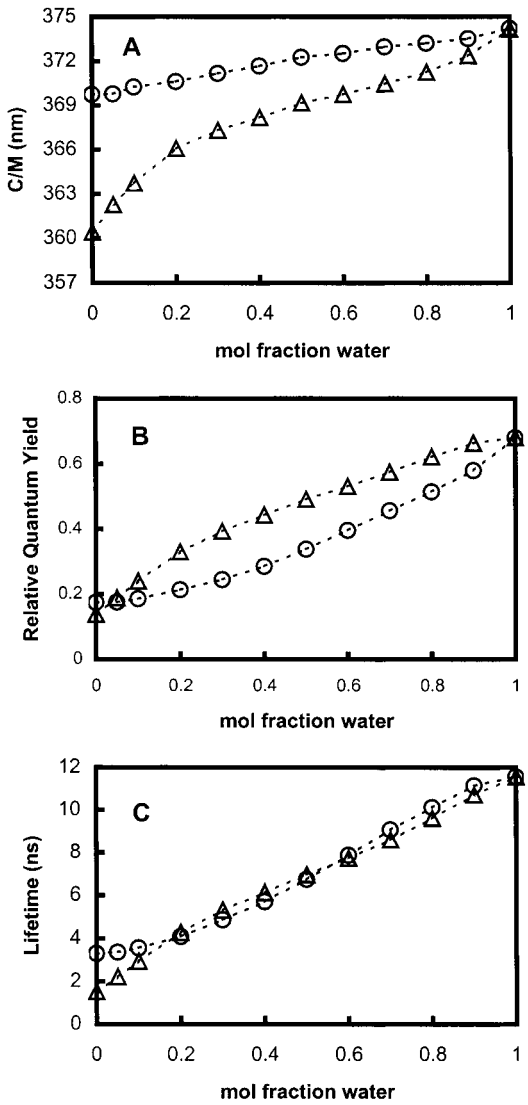

FIGURE 3: Binary solvent titrations. (A) Center-of-gravity of corrected emission spectra vs mol fraction water in dioxane (triangles) and DMF (circles); (B) Relative quantum yield of 2AP fluorescence vs mol fraction water in dioxane (triangles) and DMF (circles). The relative fluorescence values have been scaled to quantum yields assuming an absolute quantum yield of 0.68 for 2AP in water (ref 36); (C) Intensity decay lifetime vs mol fraction water in dioxane (triangles) and DMF (circles).

fluorescence changes are accompanied by changes in extinction coefficient of less than 10% (data not shown), implying that the changes in quantum yield and lifetime arise primarily from changes in nonradiative decay rates, not radiative rate constants. This discrepancy implies that approximately 30% of 2AP fluorescence is statically quenched in water but not in dioxane; the constant ratio of lifetime to quantum yield between water and DMF implies that this apparent static quenching is also present in DMF. We do not currently understand the basis for this static quenching but present two possible hypotheses. First, there could be a shift in the equilibrium between 7-H and 9-H tautomers of 2AP base due to the change in dipolar environment. The observed discrepancy between relative quantum yield and lifetime would be observed if one tautomer were statically quenched. Second, there could be a very weak specific interaction between water and 2AP that resulted in static quenching; if a specific interaction were too weak to approach saturation

at the titration endpoint, no curvature would be observed in the plot of relative quantum yield vs mol fraction water. The same effect might be observed for a relatively stronger interaction—e.g., a water-2AP hydrogen bond—that was effectively weakened by a large excess of competitor. In this scenario, the competitor would be dioxane, which might accept a hydrogen bond from water. Studies are underway to evaluate these hypotheses using the 9-methyl derivative of 2AP. This derivative exists in only one tautomeric form and can be dissolved to high concentration in a greater variety of nonpolar solvents than can the parent compound.

It may be concluded from the results depicted in Figure 3 that hydrogen bonding does not significantly alter the fluorescence properties of 2AP under the solution conditions that exist in DNA. The nearly linear dependences of emission wavelength, quantum yield, and lifetime on x_w indicate that the dominant mechanism underlying these changes is the general solvent effect. The small deviations from linearity in these parameters are similar to those that have been observed for other fluorophores in polar solvents and that have been ascribed to the effects of nonideal mixing and preferential solvation (*71*, *72*). The discrepancy between the relative quantum yield and intensity decay lifetime between dioxane and water may arise from a change in hydrogen bonding, as discussed above. However, titration from dioxane into water also causes a large shift in emission wavelength, and a corresponding spectral shift is not observed between 2AP free in water and incorporated in DNA. Therefore, neither heterogeneity of hydrogen bonding states nor transitions between those states can account for the characteristic changes in fluorescence quantum yield, lifetime, and decay kinetics that are observed for 2AP in DNA.

DISCUSSION

The fluorescence properties of 2AP incorporated into DNA exhibit characteristic features that differ from those of the free base in aqueous buffer, including decreased quantum yield and lifetime, complex intensity decay kinetics, and a small (~1 nm) shift in the emission spectrum to shorter wavelengths (*5*, *24*, *34*). Within a DNA strand, the base may undergo a variety of perturbations, including aromatic stacking and hydrogen bonding interactions, collisions with neighboring bases, and changes in solvation. Local changes in DNA conformation and dynamics due to interactions with proteins, counterions, or drugs could alter both the equilibrium thermodynamics and the kinetics of these interactions. We have investigated the effects of each of these processes on the fluorescence properties of 2AP using simple model systems.

Our results indicate that aromatic stacking of 2AP with the other DNA bases gives rise to static quenching of fluorescence and that base collisions give rise to dynamic fluorescence quenching. These two effects are not accompanied by any change in the peak wavelength or shape of the emission spectrum. The efficiencies of both static and dynamic quenching is essentially the same for all four DNA bases. At high concentrations of added base, the intensity decay becomes complex and nonexponential. These deviations from simple exponential kinetics are well-described by a modification of the theory of diffusional quenching that accounts for transient effects at high quencher concentration. The emission is also dynamically quenched with decreasing solvent polarity. This quenching is accompanied by a shift in the fluorescence spectrum to shorter wavelengths, but there is no change in the single-exponential character of the intensity decay. Hydrogen bonding affects each of the fluorescence properties negligibly.

It may be concluded from these results that all of the characteristic changes in 2AP fluorescence in DNA can be accounted for by the stacking and collisional interactions with neighboring bases. Although solvation does affect the lifetime in model systems, the absence of a significant spectral shift between water and DNA suggests that the efficiency of solvent-sensitive quenching mechanisms is essentially identical in these two environments. Furthermore, the emission wavelength, lifetime, and quantum yield are insensitive to hydrogen bonding. Therefore, only stacking and collisional interactions need be invoked to account for the fluorescence properties of 2AP in DNA and for the changes in those properties due to the structural and dynamic variation of DNA.

On the basis of this understanding of the mechanisms underlying 2AP quenching in DNA, we may construct a simple model for interpreting the results of steady-state and time-resolved fluorescence experiments. Stacking interactions will depend primarily on the equilibrium structure of a DNA molecule, which may vary significantly with nucleic acid sequence or with bound ions, drugs, or proteins. The fraction of 2AP that is stacked can be evaluated from a measurement of the extent of static quenching. Therefore, static quenching in DNA is sensitive to the local equilibrium structure. In contrast, collisions between bases will depend not only on the local equilibrium structure but also on the local and global dynamics of DNA. The effective collisional rate constant in a given DNA site can be determined by measurement of dynamic quenching of 2AP. Therefore, the average fluorescence lifetime of 2AP is a measure of both local structure and dynamics of DNA. It is convenient that the intrinsic efficiency of both static and dynamic quenching is essentially independent of the identity of the neighboring bases, because it allows fluorescence measurements to be interpreted entirely in terms of the physical properties of DNA—local structure and dynamics—rather than the specific interactions with individual bases. The utility of this approach is demonstrated in the accompanying paper in this issue, in which the extent of static and dynamic quenching of 2AP in DNA are shown to vary with both flanking sequence and DNA damage.

A family of isoxanthopterin derivatives has recently been developed as fluorescent analogues of adenine and guanine for studies of DNA (*73*−*76*). These fluorophores possess many of the same properties as 2AP, making them invaluable probes for nucleic acids. These favorable spectroscopic properties include red-shifted absorption spectra, normal or perturbed base-pairing with pyrimidines, and high quantum yield. In a series of oligos, sequence context-dependent differences in quantum yield and average lifetimes have been reported for the fluorescent guanosine analogue 3-methylisoxanthopterin (3MI) (*76*). The extent of static quenching in these oligos was found to be greater on average for 3MI flanked by purines than by pyrimidines. This observation was interpreted as evidence that static quenching of this probe might arise from stacking interactions, which might be more favorable with neighboring purines. The intensity decays

were not single exponential but required as many as four lifetime terms to fit (*76*). The average lifetimes showed no apparent correlation to the identity of the flanking bases or to any other property of the oligos. If 3MI is sensitive to collisional quenching by neighboring bases as is 2AP, the lack of sequence dependence suggests that the motions inducing these collisions are dominated by DNA dynamics that are not easily related to sequence. However, no model studies analogous to those reported here have been performed for 3MI or the other recently developed isoxanthopterin analogues. If these fluorophores were shown to respond to the same quenching interaction as 2AP does, the utility of the structural and dynamic model described above would increase because a wider range of sequences could be probed.

Understanding of the interactions between 2AP and the DNA bases would be enhanced further by a quantum mechanical description of the mechanisms underlying static and dynamic quenching. A recent excited-state calculation of 2AP and thymine with the two bases situated as though they were adjacent (same-strand) residues in B-DNA predicted a CT excitation at lower energy than the $\pi\pi^*$ excitation of 2AP (*48*). Internal conversion to this state could effectively quench the fluorescence of 2AP. By calculating the dependence of this state on base separation and orientation, it should be possible to characterize the type of geometries that are required for quenching. This insight would allow correlation of the stacking states and dynamics observed in fluorescence measurements with the structural states and molecular motions computed in molecular dynamics simulations.

The recently reported fluorescence quenching by electron transfer between 2AP and guanine in DNA may be another mechanism underlying the quenching observed in the current study (*49*). However, the quenching efficiencies reported in that study do not agree with those observed here. In the steady-state fluorescence measurements reported in the previous study, GTP was found to be 5-fold more efficient as a dynamic quencher of 2AP than the other NTPs, and no static quenching was observed with any NTP. In the current study, all the nucleosides and NTPs, including GTP, are found to be equivalent in dynamic quenching efficiency, and all are observed to cause significant static quenching. No explanation is offered for the discrepancy between these results.

Further information about the local dynamics of DNA might be obtained upon development of a mechanistic model to describe the complex intensity decay kinetics of 2AP. We hypothesize that the apparent multiexponential character of the decay may arise from modulation of the dynamic quenching rate by the internal motions of DNA. If collisions between bases originate in thermally driven vibrational fluctuations on the same time scale as fluorescence emission, then the fluorescence decay law will depend explicitly on the frequencies of those fluctuations. In this case, the observed decay would be complex and nonexponential. In fact, the molecular vibrations giving rise to collisions could be significantly faster than the apparent quenching rates, because the geometry required for the quenching interaction might only exist at large fluctuation amplitudes. Only the fraction of fluctuations that were large enough to generate that geometry would result in quenching. Therefore, if the nonexponential fluorescence decay of 2AP in DNA represents collisional quenching modulated by vibrational fluctuations, it is possible that significant information about the frequencies and character of DNA dynamics could be extracted from the time-resolved data. Interpretation of such experiments would be enhanced by computational investigations of both the quantum chemistry and macromolecular dynamics of the quenching interactions identified in the current study. Correlation of theory with 2AP fluorescence measurements could help to construct detailed molecular models of the local structural and dynamic variations of DNA.

NOTE ADDED AFTER ASAP POSTING

This article was inadvertently released ASAP on 12/30/00 before final corrections were made. Equation 6 appeared without a closing parenthesis at the end of the term. It has now been corrected in this version posted 1/23/01.

ACKNOWLEDGMENT

The authors gratefully acknowledge William R. Laws, Elena Rusinova, Eleanore Seibert, and Gintaras Deikus for helpful and stimulating discussions. In addition, we thank Edward Burstein for provision of absolute emission spectra to calculate a spectral correction curve.

REFERENCES

1. Sowers, L. C., Fazakerley, G. V., Eritja, R., Kaplan, B. E., and Goodman, M. F. (1986) *Proc. Natl. Acad. Sci. U.S.A. 83*, 5434−8.
2. Eritja, R., Kaplan, B. E., Mhaskar, D., Sowers, L. C., Petruska, J., and Goodman, M. F. (1986) *Nucleic Acids Res. 14*, 5869−84.
3. Menger, M., Tuschl, T., Eckstein, F., and Porschke, D. (1996) *Biochemistry 35*, 14710−6.
4. Stivers, J. T. (1998) *Nucleic Acids Res. 26*, 3837−44.
5. Guest, C. R., Hochstrasser, R. A., Sowers, L. C., and Millar, D. P. (1991) *Biochemistry 30*, 3271−9.
6. Baker, R. P., and Reha-Krantz, L. J. (1998) *Proc. Natl. Acad. Sci. U.S.A. 95*, 3507−12.
7. Beechem, J. M., Otto, M. R., Bloom, L. B., Eritja, R., Reha-Krantz, L. J., and Goodman, M. F. (1998) *Biochemistry 37*, 10144−55.
8. Bloom, L. B., Otto, M. R., Beechem, J. M., and Goodman, M. F. (1993) *Biochemistry 32*, 11247−58.
9. Dunkak, K. S., Otto, M. R., and Beechem, J. M. (1996) *Anal. Biochem. 243*, 234−44.
10. Fedoriw, A. M., Liu, H., Anderson, V. E., and deHaseth, P. L. (1998) *Biochemistry 37*, 11971−9.
11. Frey, M. W., Sowers, L. C., Millar, D. P., and Benkovic, S. J. (1995) *Biochemistry 34*, 9185−92.
12. Furge, L. L., and Guengerich, F. P. (1998) *Biochemistry 37*, 3567−74.
13. Goodman, M. F., and Fygenson, K. D. (1998) *Genetics 148*, 1475−82.
14. Hochstrasser, R. A., Carver, T. E., Sowers, L. C., and Millar, D. P. (1994) *Biochemistry 33*, 11971−9.
15. Jia, Y., Kumar, A., and Patel, S. S. (1996) *J. Biol. Chem. 271*, 30451−8.
16. Jia, Y., and Patel, S. S. (1997) *J. Biol. Chem. 272*, 30147−53.
17. Lam, W. C., Van der Schans, E. J., Sowers, L. C., and Millar, D. P. (1999) *Biochemistry 38*, 2661−8.
18. Reha-Krantz, L. J., Marquez, L. A., Elisseeva, E., Baker, R. P., Bloom, L. B., Dunford, H. B., and Goodman, M. F. (1998) *J. Biol. Chem. 273*, 22969−76.
19. Sastry, S. S., and Ross, B. M. (1996) *Biochemistry 35*, 15715−25.

20. Sullivan, J. J., Bjornson, K. P., Sowers, L. C., and deHaseth, P. L. (1997) *Biochemistry 36*, 8005−12.
21. Ujvari, A., and Martin, C. T. (1996) *Biochemistry 35*, 14574−82.
22. Zhong, X., Patel, S. S., Werneburg, B. G., and Tsai, M. D. (1997) *Biochemistry 36*, 11891−900.
23. Petrauskene, O. V., Schmidt, S., Karyagina, A. S., Nikolskaya, II, Gromova, E. S., and Cech, D. (1995) *Nucleic Acids Res. 23*, 2192−7.
24. Nordlund, T. M., Andersson, S., Nilsson, L., Rigler, R., Graslund, A., and McLaughlin, L. W. (1989) *Biochemistry 28*, 9095−103.
25. Lycksell, P. O., Graslund, A., Claesens, F., McLaughlin, L. W., Larsson, U., and Rigler, R. (1987) *Nucleic Acids Res. 15*, 9011−25.
26. Holz, B., Klimasauskas, S., Serva, S., and Weinhold, E. (1998) *Nucleic Acids Res. 26*, 1076−83.
27. Allan, B. W., and Reich, N. O. (1996) *Biochemistry 35*, 14757−62.
28. Allan, B. W., Beechem, J. M., Lindstrom, W. M., and Reich, N. O. (1998) *J. Biol. Chem. 273*, 2368−73.
29. Allan, B. W., Reich, N. O., and Beechem, J. M. (1999) *Biochemistry 38*, 5308−14.
30. McCullough, A. K., Dodson, M. L., Scharer, O. D., and Lloyd, R. S. (1997) *J. Biol. Chem. 272*, 27210−7.
31. Stivers, J. T., Pankiewicz, K. W., and Watanabe, K. A. (1999) *Biochemistry 38*, 952−63.
32. Thielking, V., Dubois, S., Eritja, R., and Guschlbauer, W. (1997) *Biol. Chem. 378*, 407−15.
33. Holmén, A., Nordén, B., and Albinsson, B. (1997) *J. Am. Chem. Soc. 119*, 3114−3121.
34. Evans, K., Xu, D., Kim, Y., and Nordlund, T. M. (1992) *J. Fluoresc. 2*, 209−216.
35. Smagowicz, J., and Wierzchowski, K. L. (1974) *J. Luminesc. 8*, 210−232.
36. Ward, D. C., Reich, E., and Stryer, L. (1969) *J. Biol. Chem. 244*, 1228−37.
37. Rachofsky, E. L., Sowers, L., Hawkins, M. L., Balis, F. M., Laws, W. R., and Ross, J. B. A. (1998) *Proc. SPIE 3256*, 68−75.
38. Bakhshiev, N. G. (1962) *Opt. Spectrosc. (USSR) 12*, 309−313.
39. Bilot, L., and Kawski, A. (1962) *Z. Naturforsch. A 17*, 621−628.
40. Lippert, E. (1957) *Z. Electrochem. 61*, 962−975.
41. Mataga, N., Kaifu, Y., and Koizumi, M. (1956) *Bull. Chem. Soc. Jpn. 29*, 465−470.
42. McRae, E. G. (1957) *J. Phys. Chem. 78*, 2934−2941.
43. Masaki, S., Okada, T., Mataga, N., Sakata, Y., and Misumi, S. (1976) *Bull. Chem. Soc. Jpn. 44*, 1277−83.
44. Rachofsky, E. L., Ross, J. B. A., Krauss, M., and Osman, R. (2000) *J. Phys. Chem. A* (in press).
45. Nordlund, T. M., Xu, D., and Evans, K. O. (1993) *Biochemistry 32*, 12090−5.
46. Xu, D. G., and Nordlund, T. M. (2000) *Biophys. J. 78*, 1042−58.
47. Kozlov, A. G., and Lohman, T. M. (1999) *Biochemistry 38*, 7388−97.
48. Jean, J. M., and Hall, K. B. (2000) *Biophys. J. 78*, 252A.
49. Kelley, S. O., and Barton, J. K. (1999) *Science 283*, 375−81.
50. Albert, A., and Taguchi, H. (1973) *J. Chem. Soc. (Perkins Trans.) 2*, 1101−1103.
51. Budavari, S., Ed. (1989) *The Merck Index*, Merck & Co., Rahway, NJ.
52. Lange, N. A., Ed. (1949) *Handbook of Chemistry*, 7th ed., Handbook Publishers, Inc., Sandusky, OH.
53. Lakowicz, J. R. (1999) *Principles of Fluorescence Spectroscopy*, 2nd ed., Kluwer Academic/Plenum Publishers, New York.
54. Badea, M. G., and Brand, L. (1979) *Methods Enzymol. 61*, 378−425.
55. Hasselbacher, C. A., Waxman, E., Galati, L. P., Contino, P. B., Ross, J. B. A., and Laws, W. R. (1991) *J. Phys. Chem. 95*, 2995−3005.
56. Grinvald, A., and Steinberg, I. Z. (1974) *Anal. Biochem. 59*, 583−598.
57. Bevington, P. R. (1969) *Data Reduction and Error Analysis for the Physical Sciences*, McGraw-Hill, New York.
58. Knutson, J. R., Beechem, J. M., and Brand, L. (1983) *Chem. Phys. Lett. 102*, 501−507.
59. Beechem, J. M., Knutson, J. R., Ross, J. B. A., Turner, B. W., and Brand, L. (1983) *Biochemistry 22*, 6054−6058.
60. Eftink, M. R., and Ghiron, C. A. (1981) *Anal. Biochem. 114*, 199−227.
61. Castanho, M. A. R. B., and Prieto, M. J. E. (1998) *Biochim. Biophys. Acta 1373*, 1−16.
62. Laws, W. R., and Contino, P. B. (1992) *Methods Enzymol. 210*, 448−463.
63. Bierzynski, A., Kozlowska, H., Proba, Z., and Wierzchowski, K. L. (1977) *Biophys. Chem. 6*, 231−7.
64. Bierzynski, A., Kozlowska, H., and Wierzchowski, K. I. (1977) *Biophys. Chem. 6*, 223−9.
65. Bierzynski, A., Kozlowska, H., and Wierzchowski, K. L. (1977) *Biophys. Chem. 6*, 213−22.
66. Gajewska, J., Bierzynski, A., Bolewska, K., Wierzchowski, K. L., Petrov, A. I., and Sukhorukov, B. I. (1982) *Biophys. Chem. 15*, 191−204.
67. Deranleau, D. A. (1969) *J. Am. Chem. Soc. 91*, 4044−4049.
68. Atkins, P. W. (1990) *Physical Chemistry*, 4th ed., W. H. Freeman, New York.
69. Chignell, D. A., and Gratzer, W. B. (1968) *J. Phys. Chem. 78*, 2934−2941.
70. Gryczynski, I., and Kawski, A. (1977) *Bull. Acad. Polon. Sci. (Ser. Sci. Math. Astr. Phys.) 26*, 1189−1195.
71. Suppan, P. (1987) *J. Chem. Soc. (Faraday Trans.) 83*, 495−509.
72. Khajehpour, M., and Kauffman, J. F. (2000) *J. Phys. Chem. A 104*, 7151−9.
73. Hawkins, M. E., and Balis, F. M. (2000) *Biophys. J. 78*, 306A.
74. Hawkins, M. E., Pfleiderer, W., Mazumder, A., Pommier, Y. G., and Balis, F. M. (1995) *Nucleic Acids Res. 23*, 2872−80.
75. Hawkins, M. E., Pfleiderer, W., Balis, F. M., Porter, D., and Knutson, J. R. (1997) *Anal. Biochem. 244*, 86−95.
76. Driscoll, S. L., Hawkins, M. E., Balis, F. M., Pfleiderer, W., and Laws, W. R. (1997) *Biophys J. 73*, 3277−86.

BI001664O